Nonlinear prism coupling in an organic waveguide

INFORMATION TO USERS

The most advanced technology has been used to photograph and reproduce this manuscript from the microfilm master. UMI films the text directly from the original or copy submitted. Thus, some thesis and dissertation copies are in typewriter face, while others may be from any type of computer printer.

The quality of this reproduction is dependent upon the quality of the copy submitted. Broken or indistinct print, colored or poor quality illustrations and photographs, print bleedthrough, substandard margins, and improper alignment can adversely affect reproduction.

In the unlikely event that the author did not send UMI a complete manuscript and there are missing pages, these will be noted. Also, if unauthorized copyright material had to be removed, a note will indicate the deletion.

Oversize materials (e.g., maps, drawings, charts) are reproduced by sectioning the original, beginning at the upper left-hand corner and continuing from left to right in equal sections with small overlaps. Each original is also photographed in one exposure and is included in reduced form at the back of the book. These are also available as one exposure on a standard 35mm slide or as a 17" x 23" black and white photographic print for an additional charge.

Photographs included in the original manuscript have been reproduced xerographically in this copy. Higher quality 6" x 9" black and white photographic prints are available for any photographs or illustrations appearing in this copy for an additional charge. Contact UMI directly to order.

UMI

University Microfilms International
A Bell & Howell Information Company
300 North Zeeb Road, Ann Arbor, MI 48106-1346 USA
313/761-4700 800/521-0600

Order Number 1335694

Nonlinear prism coupling in an organic waveguide

Keilbach, Kevin Anthony, M.S.

The University of Arizona, 1988

U·M·I
300 N. Zeeb Rd.
Ann Arbor, MI 48106

NONLINEAR PRISM COUPLING IN AN ORGANIC WAVEGUIDE

by

Kevin Anthony Keilbach

A Thesis Submitted to the Faculty of the

COMMITTEE on OPTICAL SCIENCES (Graduate)

In Partial Fulfillment of the Requirements
For the Degree of

MASTER OF SCIENCE

In the Graduate College

THE UNIVERSITY OF ARIZONA

1 9 8 8

STATEMENT BY AUTHOR

This thesis has been submitted in partial fulfillment of requirements for an advanced degree at The University of Arizona and is deposited in the University Library to be made available to borrowers under rules of the Library.

Brief quotations from this thesis are allowable without special permission provided that accurate acknowledgment of source is made. Requests for permission for extended quotation from or reproduction of this manuscript in whole or in part may be granted by the head of the major department or the Dean of the Graduate College when in his or her judgment the proposed use of the material is in the interests of scholarship. In all other instances, however, permission must be obtained from the author.

SIGNED: Kevin Anthony Kelbach

APPROVAL BY THESIS DIRECTOR

This thesis has been approved on the date shown below:

G. I. Stegeman
Professor of Optical Sciences

Dec. 13, 1988
Date

ACKNOWLEDGEMENT

My deepest thanks to Ray Zanoni for his late nights, advice and help that enabled me to finish this thesis and for being a good friend. I also wish to thank the guys in the lab for all their help; William Torruellas for help to make the laser work, Kent Rochford for his help and advice on how to guide light in a film with prism couplers, Gaetano Assanto for his help with the numerical analysis sections, and all those others who gave me equipment, advice or just made it fun; Gill, Francis, Mark, Bill, Victor, Pat, Brian, Ken, Kelly, Jeff, Li, Alain, Quain, Suk. I also wish to thank Professor George Stegeman without whose help none of this would have been possible.

Finally, I thank my parents, Joseph and Elizabeth, for their encouragement and support throughout my academic career.

TABLE OF CONTENTS

LIST OF ILLUSTRATIONS

ABSTRACT

Computer modeling of prism coupling of pulsed laser irradiation at a wavelength of 1064 nm into an organic polymer waveguide with Kerr Law nonlinearities showed that the prism coupling technique has inherent problems that make it difficult to accurately determine the magnitude of the refractive index change. Uncertainty in knowledge of the gap spacing under the prism leads to errors in any estimates of these nonlinear refractive index changes. Results from prism coupling experiments conducted on a polymer waveguide with a pulsed laser are inconclusive.

CHAPTER ONE

INTRODUCTION

Guided wave optical devices offer potentially significant increases in speed and performance over analogous electronic circuits for applications such as communications or computing (Smith, 1982; Potember et al., 1988). The quest for a viable all optical transistor allowing modulation of light with light with large fan-in and fan-out capabilities and low power requirements continues at an accelerated pace throughout the world. The primary obstacle to building such a device is the identification of a material that exhibits large nonlinear optical effects with high speed and low power consumption (Smith, 1982; Stegeman et al., 1988; Potember et al., 1988; Munn, 1988). A variety of material systems, ranging from semiconductors to glasses to polymers etc. have been, and are being considered in various device geometries. To date the "ideal" material has not yet been identified and much work needs to be done to overcome these material limitations if suitable nonlinear optical devices are to be made (Stegeman et al., 1987, 1988). The development of simple techniques for quantifying intensity dependent refractive indices in waveguides is necessary in the search for a suitable material.

Nonlinear optical effects based on intensity dependent refractive index changes have generated much interest because of their applications to optical devices for communications which require that there be no frequency shift from the input frequency. To understand the basic physics behind these nonlinear effects, it is useful to first consider the wave equation in a dielectric medium (Shen, 1984; Hopf & Stegeman, 1985):

$$- \nabla^2 \mathbf{E} + \nabla(\nabla \cdot \mathbf{E}) = -\mu_0 \frac{\partial^2 \mathbf{P}}{\partial t^2} \quad (1.1)$$

where **E** is the applied field and **P** is the polarization induced in the material. The dielectric polarization tensor, **P**, can be written as a Taylor series expansion in the applied field:

$$P(\omega_i,k_i) = \epsilon_0[\chi^{(1)} + \chi^{(2)}:E(\omega_k,k_k) + \chi^{(3)}:E(\omega_k,k_k)E(\omega_l,k_l) + \ldots]E(\omega_j,k_j) \quad (1.2)$$

where i,j,k,l denote the different frequency and wavevector components of the incident and generated fields. Various optical phenomena can be attributed to each of the terms on the right hand side in the above equation. The first term represents linear optical effects and is responsible for the linear index of refraction and for absorption. Elements of the $\chi^{(2)}$ tensor are responsible for such nonlinear processes as second harmonic generation, parametric mixing, and optical rectification, and it can be proven that materials exhibiting such effects must have a noncentrosymmetric molecular structure. Materials with large $\chi^{(2)}$ values have found widespread commercial applications as frequency doublers for lasers. Much promise lies in materials with large fast $\chi^{(3)}$ values. Nonlinear processes such as third harmonic generation, four-wave mixing, two-photon absorption, phase conjugation and intensity dependent refractive index changes or Kerr Law effects all result from interactions of the applied field with various components of the $\chi^{(3)}$ matrix. These intensity dependent refractive index changes can be used to make switchable all-optical devices.

The magnitude of the refractive index changes for a material that obeys the Kerr Law response depends on the strength of the input intensity. The

refractive index for a Kerr material is given by (Shen, 1984; Hopf & Stegeman, 1985; Carter et al., 1987):

$$n = n_0 + n_2 I \tag{1.3}$$

where n_0 is the linear index, I is the local intensity in a material and n_2 is the coefficient for the intensity dependent index which for homogeneous and isotropic materials is proportional to the $\chi^{(3)}$ of the material. Since the magnitude of the index change is also proportional to the local intensity, waveguides, with their inherently small beam cross section and diffractionless propagation for long distances make excellent geometries for studying these nonlinear effects (Smith, 1982; Stegeman et al., 1987, 1988). Several integrated optical device designs exist employing these nonlinear index change effects. (Stegeman et al., 1987, 1988) Therefore measurements in a waveguide geometry are thus an effective means of quantifying material parameters to determine their usefulness for integrated optical devices.

Extensive research has been conducted to identify useful nonlinear materials. Semiconductors and semiconductor doped glasses show high nonlinearities and several devices have already been demonstrated in these materials. Semiconductors, however, suffer from high absorption and propagation losses in semiconductor waveguides are relatively high (Stegeman et al., 1987, 1988). Organic polymers, on the other hand, show large non-resonant $\chi^{(3)}$ values and extremely fast response times. Currently much commercial interest exists in developing polymers for device applications. Polymer chemistry is well-understood making it possible to optimize material properties for waveguide device

requirements. The ideal organic material will show large nonlinearities with low absorption at a usable wavelength, and should be easily processible into low loss waveguides (Smith, 1982; Stegeman et al., 1987, 1988; Burzynski et al., 1988). A technique to quantify polymer properties in waveguide form needs to be developed.

Prism (and grating) coupling into thin film waveguides has become a popular technique for studying nonlinear optical effects in planar waveguides. The relative ease with which it is possible to prepare a prism-coupler apparatus makes the method especially attractive. The purpose of this thesis is to assess prism coupling as a technique for studying the nonlinear optical effect of intensity dependent refractive index changes in planar waveguides made from organic materials. The basic physics of linear waveguides and of prism coupling into linear waveguides is presented. Modifications to this theory for waveguides made of materials displaying an intensity dependent index of refraction are discussed. Numerical results outlining problems in setting waveguide geometry and the effects on error in values found for nonlinearities using prism coupling techniques are presented. Experimental results for prism coupling into one polymer are given and overall problems with the technique are discussed.

CHAPTER TWO

WAVEGUIDE AND DISTRIBUTED COUPLER THEORY

There are two approaches used in the literature to describe the propagation of modes in planar waveguides. Following the analysis of Kogelnik (Kogelnik, 1975) light propagation in a planar slab waveguide can be easily explained using ray optics. Consider the asymmetric waveguide shown in figure 2.1. Light propagating in a waveguide will follow a zig-zag path provided that the angle of incidence at each interface is greater than the critical angle so that total internal reflection occurs. This requires that the indices of refraction for each medium satisfy the conditions $n_f > n_s$ and $n_f > n_c$. As a further constraint, constructive interference must occur on successive reflections and the light propagates in slab waveguides only in discrete modes where the round-trip travel between each interface introduces only an integral multiple of 2π phase change.

A rigorous discussion of waveguide modes involves employing Maxwell's equations for electromagnetic wave propagation. Consider the relations for source free, time dependent fields:

$$\nabla \times E(t) = - \frac{\partial B(t)}{\partial t}$$
$$\nabla \times H(t) = \frac{\partial D(t)}{\partial t} \qquad (2.1)$$

where E(t), H(t) and D(t), B(t) are the time dependent electric and magnetic field vectors in free space and in a material respectively, and are given as

$$E(t) = \frac{1}{2}E \exp(j\omega t) + c.c.$$
$$H(t) = \frac{1}{2}H \exp(j\omega t) + c.c. \qquad (2.2)$$

and

$$D(t) = \epsilon E(t)$$
$$B(t) = \mu H(t)$$

Here ϵ and μ are the scalar dielectric constant and scalar magnetic permeability respectively of a lossless medium. The boundary conditions at the material interfaces are given by:

$$e_n (\cdot) (B_1 - B_2) = 0 \qquad e_n (\cdot) (D_1 - D_2) = 0$$
$$e_n \times (E_1 - E_2) = 0 \qquad e_n \times (H_1 - H_2) = 0 \qquad (2.3)$$

where e_n denotes a unit vector normal to the material interface and the subscripts 1 and 2 refer to materials 1 and 2 above and below the interface. It turns out to be convenient to define a coordinate system such that the fields in a waveguide have components in the transverse and longitudinal directions (denoted by t and x respectively) then:

$$E = E_t + E_x \qquad H = H_t + H_x \qquad (2.4)$$

The propagation constant of the ν'th waveguide mode is defined by:

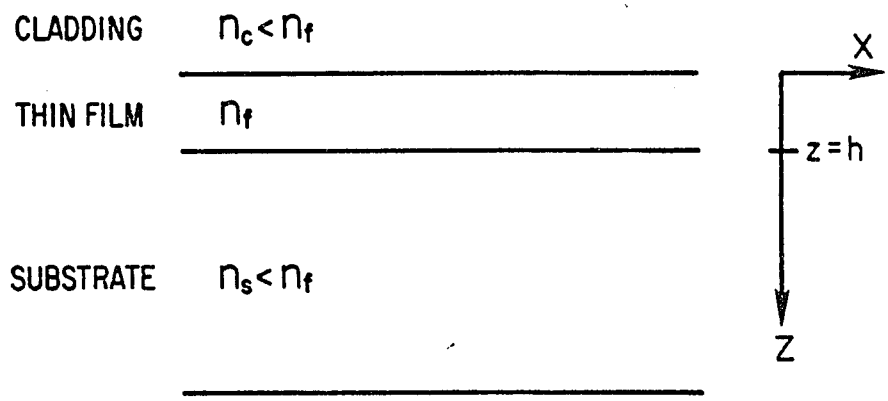

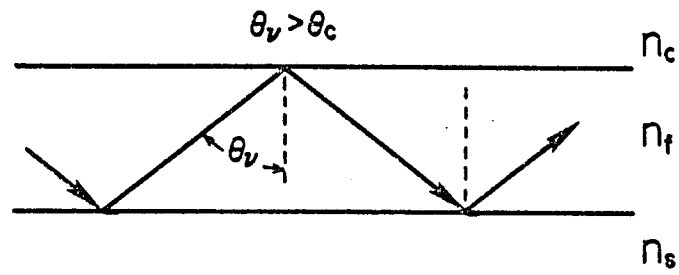

Figure 2.1. Asymmetric planar-slab waveguide geometry.

$$\beta_\nu = n_f\, k_0 \sin\theta \tag{2.5}$$

where k_0 is the free space wavevector and θ is the angle of incidence at the film interfaces.

The allowed waveguide modes can easily be found by using the solutions to Maxwell's equations, subject to the boundary conditions at both film interfaces. The guided wave fields can be expanded in terms of the waveguide modes as:

$$E(x,y,z) = \sum_\nu \frac{1}{2} E_\nu\,(y,z)\, e^{-j\beta_\nu x} + \text{c.c.} \tag{2.6}$$

$$H(x,y,z) = \sum_\nu \frac{1}{2} H_\nu\,(y,z)\, e^{-j\beta_\nu x} + \text{c.c.} \tag{2.7}$$

Using equations 2.1, 2.2 and 2.4 - 2.7, Maxwell's equations for a waveguide mode are written as

$$\nabla_t \times E_{t\nu} = -j\omega\mu H_{x\nu} \qquad \nabla_t \times H_{t\nu} = j\omega\epsilon E_{x\nu} \tag{2.8}$$

$$\nabla_t \times E_{x\nu} - j\beta_\nu\, e_x \times E_{t\nu} = -j\omega\mu H_{t\nu} \tag{2.9}$$

$$\nabla_t \times H_{x\nu} - j\beta_\nu\, e_x \times H_{t\nu} = j\omega\epsilon E_{t\nu} \tag{2.10}$$

If light is confined in only one dimension (i.e., the z direction), as is the case with a planar slab waveguide, then equations 2.8 - 2.10 can be further simplified. Modal solutions show either transverse electric (TE, $E_x = 0$) or transverse magnetic

(TM, H_x=0) field solutions. The wave equation for TE modes is given by:

$$\frac{\partial^2 E_y}{\partial z^2} = (\beta_\nu{}^2 - n^2 k_0{}^2) E_y \tag{2.11}$$

(A similar equation results for TM modes). Application of the boundary conditions 2.3 ($\partial E_y/\partial z$ and H_x continuous) at the material interfaces z = 0 and z = h gives field solutions in each medium as:

$$E_y = E_c\, e^{\gamma_c z} \qquad \text{for } z < 0 \qquad \text{Cover} \tag{2.12}$$

$$E_y = E_f \cos(\kappa_f z - \phi_c) \qquad \text{for } 0 < z < h \qquad \text{Film} \tag{2.13}$$

$$E_y = E_s\, e\text{^}(-\gamma_s (z-h) \qquad \text{for } h < z \qquad \text{Substrate} \tag{2.14}$$

where

$$\gamma_c^2 = \beta^2 - n_c{}^2\, k_0{}^2 \tag{2.15}$$

$$\kappa_f^2 = n_f{}^2\, k_0{}^2 - \beta^2 \tag{2.16}$$

$$\gamma_s^2 = \beta^2 - n_s{}^2\, k_0{}^2 \tag{2.17}$$

Modes propagating in the x direction in an asymmetric waveguide consist of oscillatory field solutions in the guiding film and exponentially decaying or evanescent field solutions in the cover and substrate. The phase shift on reflection at each interface is found from boundary conditions 2.3 to be:

$$\tan \phi_s = \frac{\gamma_s}{\kappa_f} \qquad \tan \phi_c = \frac{\gamma_c}{\kappa_f} \tag{2.18}$$

For a guided mode the total phase shift for one round trip propagation between

the two interfaces must be an integer multiple of 2π. Thus the dispersion relation is:

$$\kappa_f \, h - \phi_s - \phi_c = \nu\pi \tag{2.19}$$

Field solutions to this equation result in propagating modes within the film waveguide.

Light can be injected into a waveguide via either a prism or a grating coupler. Consider using a prism of index n_p separated from the thin film by a gap of index n_a to couple light into a planar waveguide as shown in figure 2.2. If the condition for the total internal reflection of light incident onto the prism base ($\theta > \theta_c = \sin^{-1} (n_a/n_p)$) is satisfied then the sum of the incident and reflected waves gives a standing wave field pattern along the vertical direction inside the prism and an exponentially decaying field below the prism base. This prism field propagates in the horizontal x direction. The evanescent field below the prism can couple weakly to a guided mode of the film waveguide in the cover, as given by equation 2.12. Fields in-coupled at the base of the prism propagate in the waveguide and interfere with fields in-coupled at each successive point under the prism. If the interference between these fields is constructive, the guided wave amplitude grows. Maximum energy transfer between the prism and guide will occur provided that the phase match condition:

$$n_p \, k_0 \sin\theta = \beta_{gw} \tag{2.20}$$

is satisfied and the input beam waist to prism interaction length ratio is optimized.

Given a uniform space between prism and film, it is theoretically possible to couple energy into a waveguide with a prism with η = 80% efficiency.

A more rigorous approach to prism coupling involves considering the input beam temporal and spatial profiles and the waveguide geometry. Following the approach of Ulrich (Ulrich, 1970; Assanto et al., 1988) the incident and guided-wave fields are given by:

$$E(r,t) = \frac{1}{2}\,\hat{e}_{in}\; a_{in}(x,t)\exp\{j[\omega t - n_p\; k_0(\sin\theta x - \cos\theta z\;)]\} + c.c.$$

$$E(r,t) = \frac{1}{2}\,\hat{e}_{gw}\; a_{gw}(x,t)f(z)\exp\{j[\omega t - \beta(x,t)x]\} + c.c. \qquad (2.21)$$

and the coupled wave equation for a lossy waveguide is just:

$$\frac{\partial}{\partial x}\, a_{gw}\,(x) = \hat{t}\; a_{in}\;(x)\; e^{j\;\phi_0(x,t)} - \left[\alpha_{att} + \frac{1}{l_c}\right] a_{gw}\;(x) \qquad (2.22)$$

$$\phi_0(x,t) = [\beta(x,-\infty) - n_p\; k\; \sin\theta]x \qquad (2.23)$$

where f(z) is the transverse field distribution, $a_{gw}(x)$ is a complex amplitude term describing the guided wave field, $a_{in}(x)$ describes the incident field, $\hat{t}$ is the transfer function for the coupling geometry, α_{att} is the attenuation coefficient for the waveguide, l_c is the characteristic length for reradiation into the prism from a guided wave, and $\phi_0(x,t)$ reflects any phase mismatch between the guided mode and the input. Equation 2.22 relates the field incident on the prism base to the guided-wave field. It simply shows that the guided-wave power will grow under the prism subject to the waveguide geometry and that losses will be due to

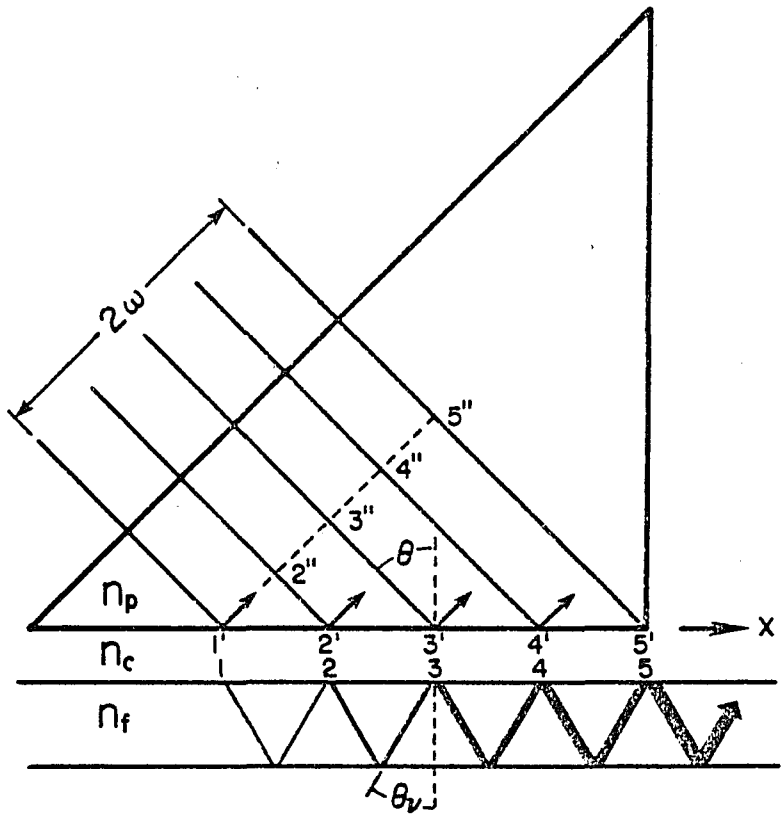

Figure 2.2. Prism-coupling into a thin film waveguide.

absorption and scattering in the waveguide, and reradiation into the prism.

Prism Coupling into Nonlinear Waveguides

If the film waveguide in the above analysis is given an intensity dependent index of refraction such that:

$$n_f = n_0 + n_2 I \tag{1.3}$$

the guided wave vector β_{gw} for the ν^{th} mode will be power dependent such that:

$$\beta_{gw} = \beta_0 + \Delta\beta(P)$$
$$\Delta\beta(P) = \beta_2 P_{gw} \tag{2.24}$$

where P_{gw} is the guided-wave power (Liao et al., 1985; Assanto et al., 1988; Fortenberry et al., 1988). From equation 2.20, the projection of the incident wavevector onto the prism base equals the guided wavevector β_{gw} for efficient coupling. When the waveguide contains a material with an intensity dependent index of refraction, the coupling efficiency becomes power dependent.

The above linear coupling analysis can be extended to the nonlinear case using the methods of Assanto, et al (Assanto et al., 1988) for prism coupling into films exhibiting a power dependent β_{gw} . The coupled mode equation 2.22 becomes:

$$\frac{\partial}{\partial x} a_{gw}(x,t) = \hat{t}\, a_{in}(x,t)\, e^{j\Phi(x,t)} - \left[\alpha_{att}(x,t) + \frac{1}{l_c}\right] a_{gw}(x,t) \tag{2.25}$$

where now equation 2.23 becomes:

$$\Phi(x,t) = \phi_0(x,t) + \phi^{NL}(x,t) \tag{2.26}$$

where $\phi^{NL}(x,t)$ is the power dependent nonlinear phase term. At low powers $\phi^{NL}(x,t)$ is negligible and the phase match condition is identical to that found in the linear case. If the prism coupler is optimized for maximum coupling efficiency at low power, and the power is increased, $\phi^{NL}(x,t)$ will not be negligible and the phase match condition will no longer be valid. Hence the coupling efficiency decreases with the guided-wave power (Assanto et al., 1988; Fortenberry et al., 1988).

The magnitude of the nonlinear phase change is determined by the nature of the nonlinearity and the material being considered. Two general categories of nonlinearities are expected to contribute to index changes in a waveguide: 1) electronic or Kerr Law nonlinearities for which the index change is directly dependent on the intensity; and 2) thermal nonlinearities for which index changes are dependent on the local temperature change within the material due to absorption. Electronic nonlinearities that lead to index changes result from the interaction of the applied field with elements of the $\chi^{(3)}$ tensor. Thermal index changes are influenced by a materials ability to absorb, store, and dissipate heat. The thermal index change coefficient is given by (Assanto et al., 1988):

$$n_{2\text{thermal}} = \frac{\partial n}{\partial T} \frac{\alpha_0 \tau_t}{\rho C_p} \tag{2.27}$$

where α_0 is the linear absorption coefficient, ρ is the density, τ_t is the thermal relaxation time, ∂T is the local temperature rise in the material, and C_p is the heat capacity. The total intensity dependent index change is just the superposition of these effects and the total nonlinear phase shift is given by (Assanto et al., 1988):

$$\frac{\partial}{\partial x}\,\phi^{NL}\,(x,t) = \Delta\beta_{elec}(x,t) + \Delta\beta_{thermal}\,(x,t) \tag{2.28}$$

Thermal nonlinearities tend to have much slower relaxation times than electronic nonlinearities due to slow thermal diffusion. For polymeric materials, the electronic response may be on the order of several hundred femtoseconds while the thermal response may be measured in microseconds. Consequently, if a sample is illuminated with a pulse several nanoseconds long, index changes due to electronic nonlinearities will follow the intensity profile of the pulse while thermal effects will integrate over the pulse profile. An effective thermal $n_{2,eff}$ results from this integration and is the calculated n_2 from equation 2.24 reduced by the ratio of the laser pulse width, Δt, to the material thermal relaxation time, τ_t:

$$n_{2eff} \cong n_2\,\frac{\Delta t}{\tau_t} \tag{2.29}$$

Thermal nonlinearities, also termed integrating nonlinearities, can cause distortions of the input pulse that give insight into the nature of the nonlinearities in a thin film waveguide (Assanto et al., 1988; Fortenberry et al., 1988).

In practice, coupling into a thin film to study the nonlinear properties is not as straightforward as this analysis makes it appear. The geometrical transfer function $\hat{t}$ contains information on many coupling parameters of the waveguide that must be optimized to prevent degradation of the coupling efficiency. Because it is difficult to optimize these factors it is useful to study how other than optimum values will effect waveguide coupling efficiency.

CHAPTER THREE

NUMERICAL ANALYSIS OF PRISM COUPLING

The accuracy with which the nonlinear index can be obtained with the prism coupling technique is questionable. Factors such as the gap spacing, h_g, input beam position with respect to prism edge, x_s, (see figure 3.1) and beam waist, w_0, may be difficult to control or may simply not be known. It is, therefore, useful to develop a numerical model to study how variations in these parameters will affect the guided wave power in a prism coupler.

The coupled wave theory of chapter 2 for prism coupling of pulses into a waveguide with an intensity dependent index of refraction is incorporated in a Fortran computer code running on a Sun Microsystems Computer (unpublished work of Stegeman and Zanoni, 1987). Coupling of 18 ns (FWHM) pulses of Gaussian temporal profile at a wavelength of 1.064 μm into a planar waveguide able to support a TE_0 mode is modeled. Pulses propagating in the waveguide are assumed to be of Gaussian spatial extent in the x-direction and of infinite extent in the y-direction. Typical conservative values for electronic and thermal n_2 are assumed. Coupling efficiency at low power is maximized for a given set of conditions and the input power incident on the prism base is slowly incremented. Variation of the coupling efficiency with input power for the various parameters is studied.

Figure 3.2 shows a drop-off of the coupling efficiency with increasing pulse energy from the theoretical 80% maximum for comparable values of integrating and electronic nonlinearities. With all of the coupling parameters optimized, both

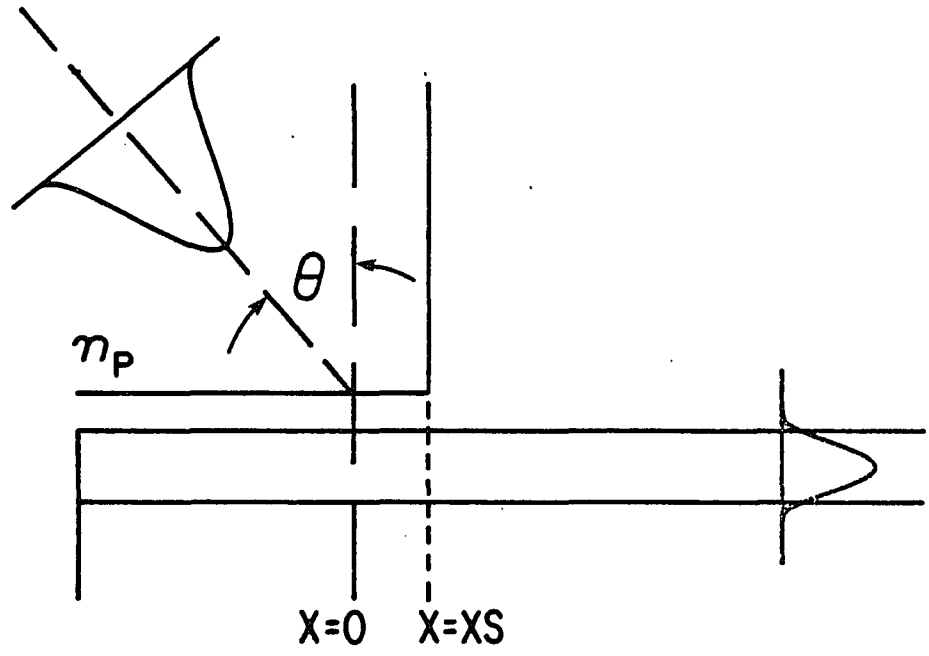

Figure 3.1. Geometry for prism-coupling of a Gaussian beam into a thin film waveguide. Prism edge, xs; beam angle of incidence at prism base, θ; gap spacing, h_g; prism index, n_p.

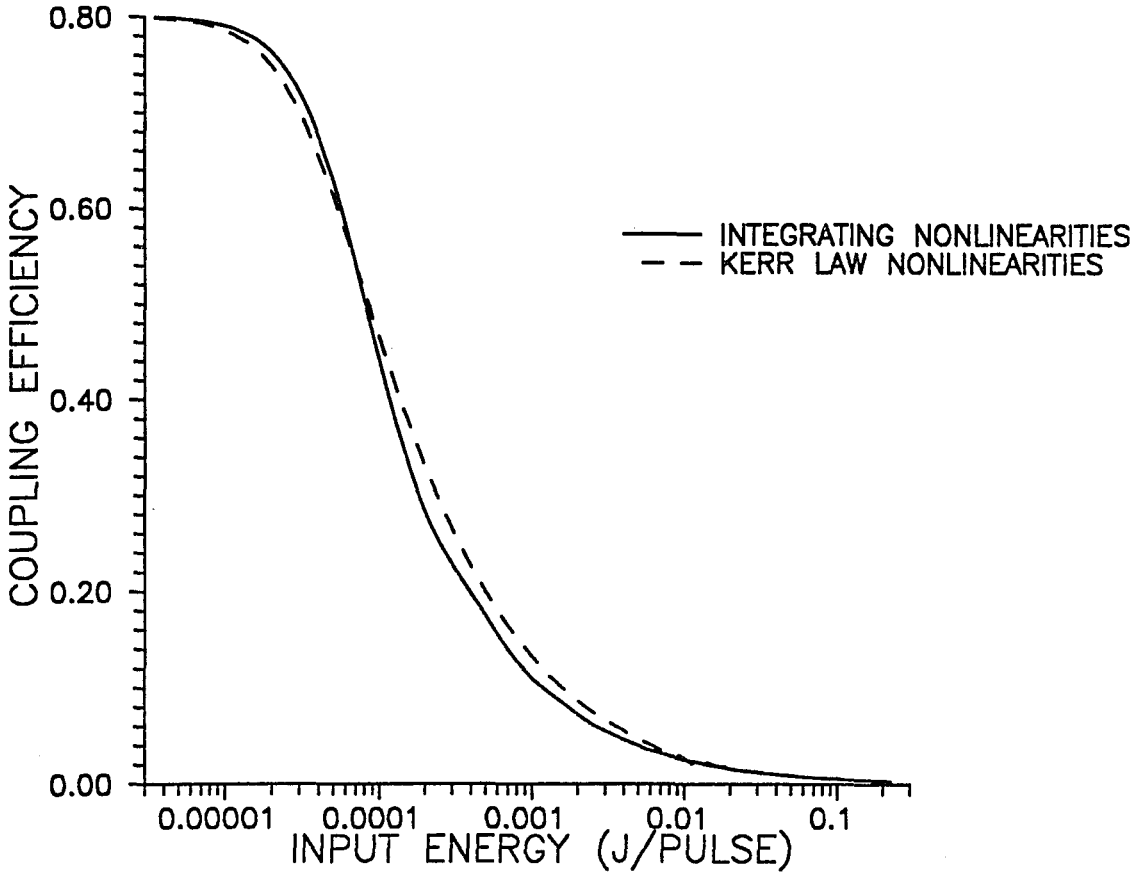

Figure 3.2. Coupling efficiency versus input energy for optimum coupling conditions and uniform gap for Kerr law and integrating nonlinearities.

electronic and integrating nonlinearities give nearly identical efficiency reductions. Differences in the two curve indicate that electronic effects are slightly more sensitive to incident energy changes than are thermal effects.

Figure 3.3 shows the variation in the coupling efficiency for several values of detuning considering only electronic nonlinearities. Detuning is defined as the deviation of the input condition from the synchronous coupling condition and is given by

$$\text{Detuning} \equiv (\beta_{gw}(x,-\infty) - n_p k_0 \sin\theta_{inc})\ 2w_0 \tag{3.1}$$

where w_0 is the beam waist. The curves indicate that detuning (by changing θ_{inc}) shifts the power for maximum efficiency. For positive detuning the maximum efficiency shifts to higher powers. As the guided wave power increases the index changes until, at some point, the synchronous coupling condition is satisfied somewhere under the prism and the efficiency is maximized. This effect becomes quite pronounced for large detuning values where the film index at the prism base changes with power until the waveguide switches on and the efficiency rises to a maximum. Further increases in power changes the index and again violates the synchronous coupling condition. The efficiency decreases.

Figure 3.4 shows that for a given beam waist the efficiency is strongly dependent on the coupling gap spacing, h_g. This represents the largest source of error when considering the prism coupling technique as an analytical technique for evaluating nonlinearities. With a prism-coupled waveguide it is difficult to specify or measure the gap spacing. Small particles or slight variations in the film thickness under the prism prevent the gap from being explicitly specified and

mechanical problems in mounting the prisms prevent a uniform gap from forming. Uncertainty of the gap size represents a serious problem in using prism coupling as an analytical technique for finding material nonlinearities.

Figure 3.5 demonstrates how, for a given n_2 and beam waist, variation of the gap size affects the efficiency. For large detuning, variation of the gap not only changes the magnitude of the coupling efficiency, but also the energy at which the maximum efficiency for a given gap size occurs. Denoting this pulse energy for peak efficiency for a particular gap as $E_0(h_g)$, $E_0(h_g)$ varies under the efficiency curve for the optimum gap. The peak efficiency is a maximum when the gap is set to its optimum value and there $E_0(h_g)$ has its smallest value. If the gap size is other than the optimum value, $E_0(h_g)$ will be larger for a given n_2. Figure 3.6 shows this to be the case as n_2 varies over several orders of magnitude. Values for n_2 versus $E_0(h_g)$ from this graph are plotted in Figure 3.7. Each line represents a curve of constant gap and the family of curves gives a indication of the error in any estimate of n_2 with uncertainties in the gap size. Thus, because it is impossible to determine a gap size, any n_2 value found by assuming a gap size will be in error by a factor proportional to the error in the gap size. A conservative experimentalist will always assume an optimum gap so that, for a given $E_0(h_g)$, the estimate of n_2 will be less than or equal to the true value. For example, if $E_0(h_g)$ is found to be 0.001 [J/pulse] then the smallest estimate of n_2 will be $\cong$ 3.2 x 10^{-17} [m^2/w] for the optimum gap of 0.18 μm. If this gap is not optimized the actual n_2 value will be larger than this estimate. Thus, if upper and lower bounds can be placed on any assumptions about gap size then n_2 can be estimated to within a certain range.

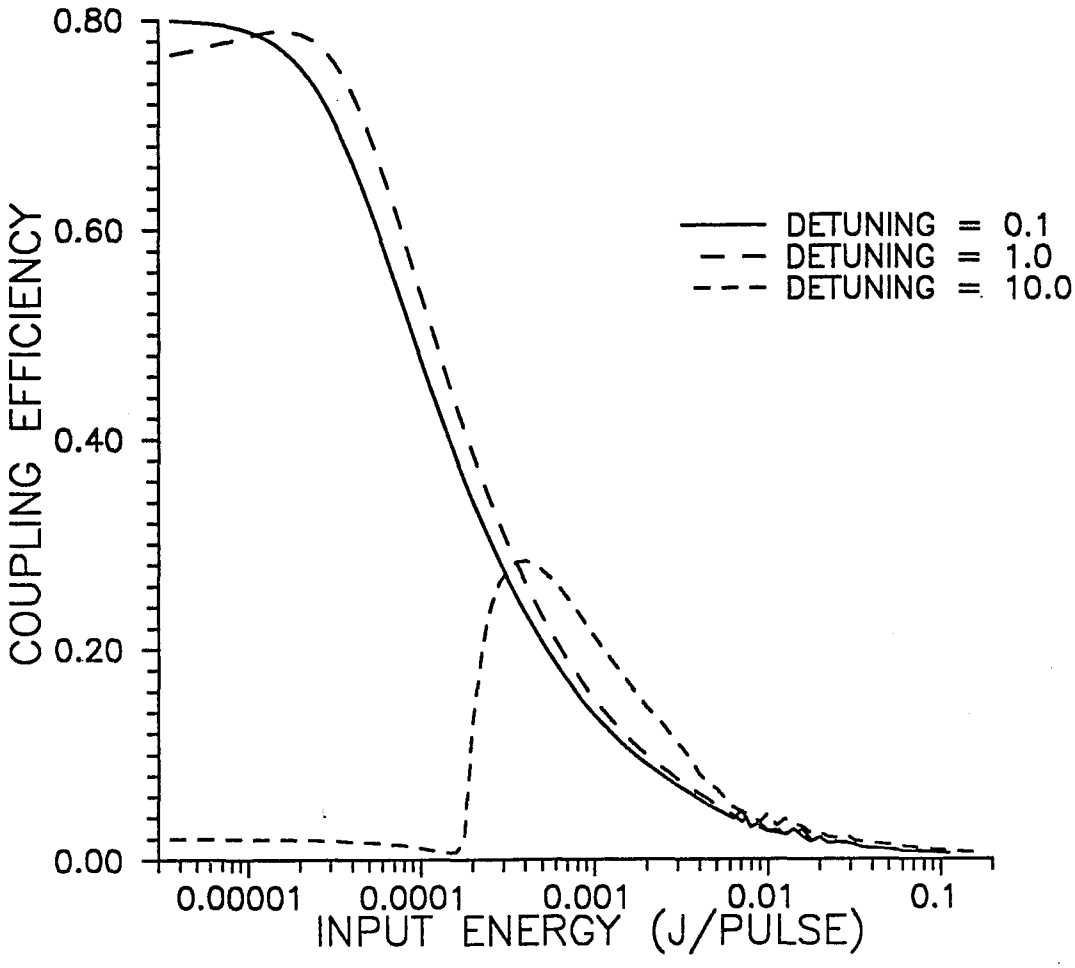

Figure 3.3. Coupling efficiency versus input energy for optimized gap and detuning of 0.1, 1.0, and 10.0 with Kerr law nonlinearities.

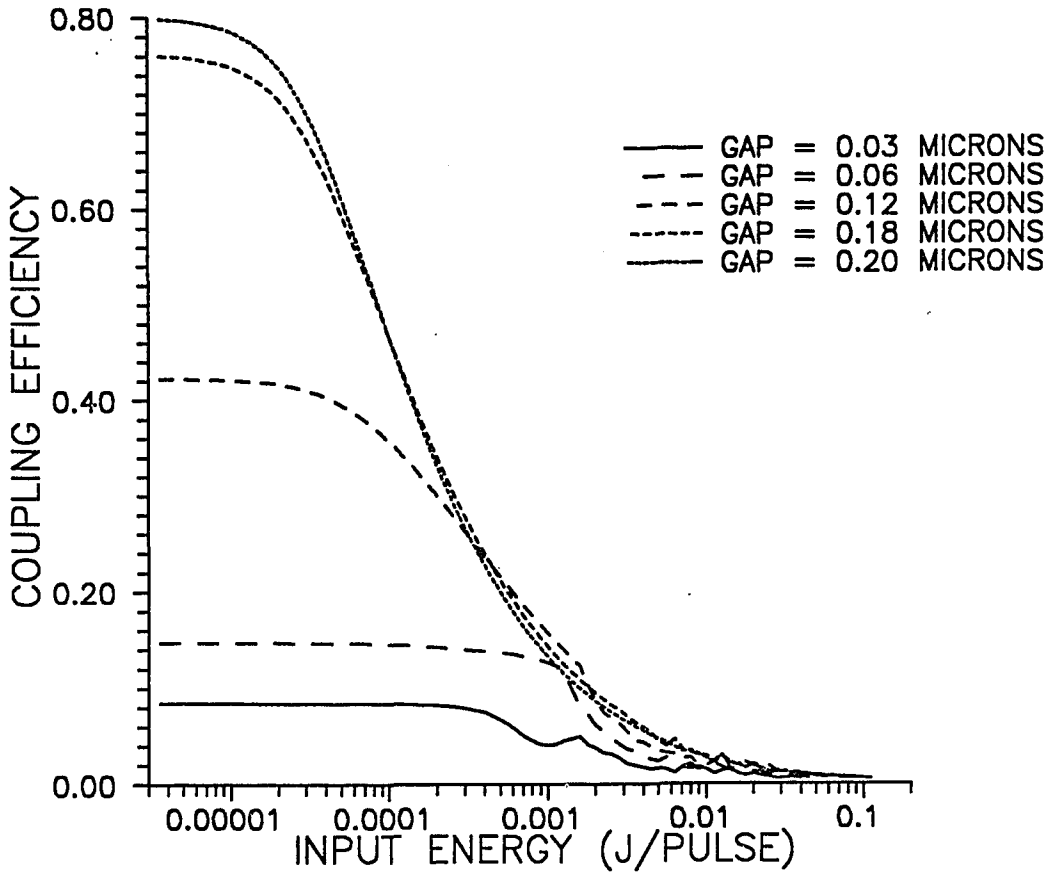

Figure 3.4. Coupling efficiency versus input energy for zero detuning and gap spacings of 0.03 μm, 0.06 μm, 0.09 μm, 0.12 μm, 0.18 μm, and 0.20 μm. with Kerr law nonlinearities.

Additional computer runs indicated that variation of the input beam offset with respect to the prism edge from the optimum value of 0.72 w_0 affects the coupling efficiency only negligibly. It should be possible to set the beam position near the optimum value so that degradation of the coupling efficiency due to this factor should be negligible.

Modeling of prism coupling into waveguides has given insight into the dependence of the waveguide output on the geometric coupling parameters of the guide. Provided that the beam waist at the prism base is well characterized these parameters are, in theory, all that contribute to degradation of the coupling efficiency. This analysis shows that uncertainty in the gap size leads to a significant error in the estimate of n_2. In practice many other problems arise that may make prism coupling less desirable than other techniques.

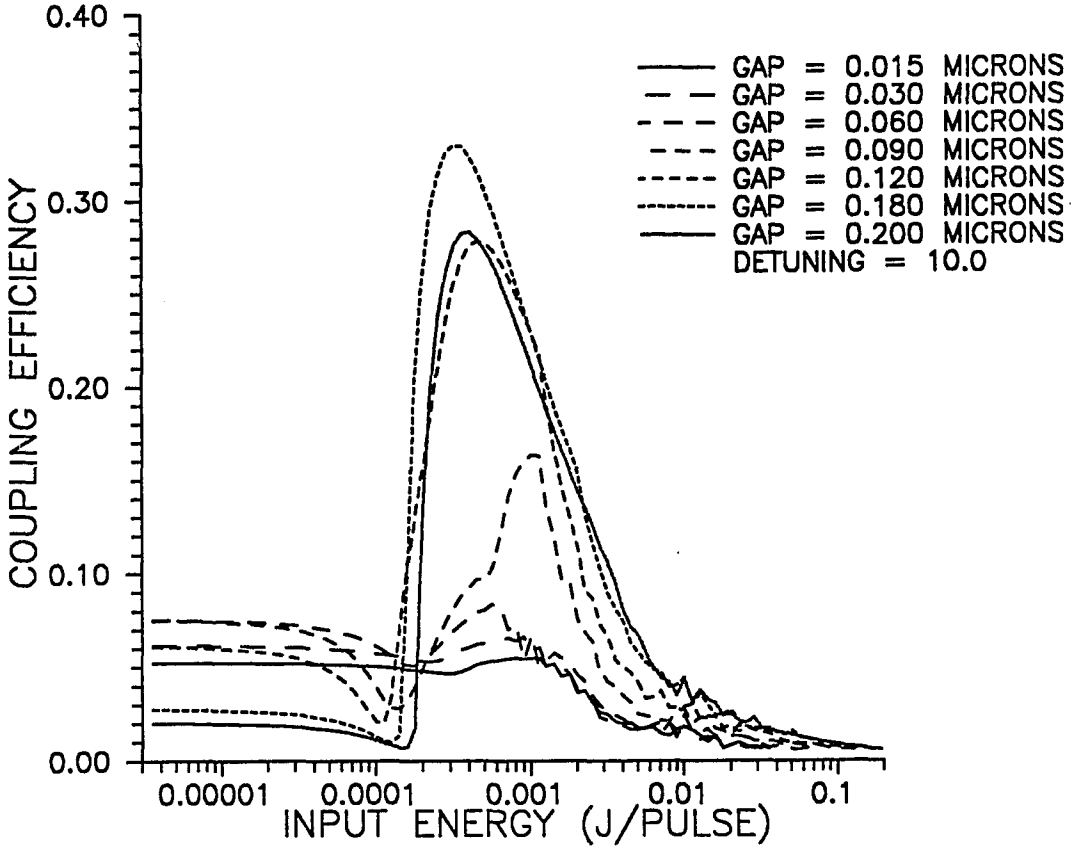

Figure 3.5. Coupling efficiency versus input energy for detuning of 10.0 and gap spacings of 0.03 μm, 0.06 μm, 0.09 μm, 0.12 μm, 0.18 μm, and 0.20 μm with Kerr law nonlinearities.

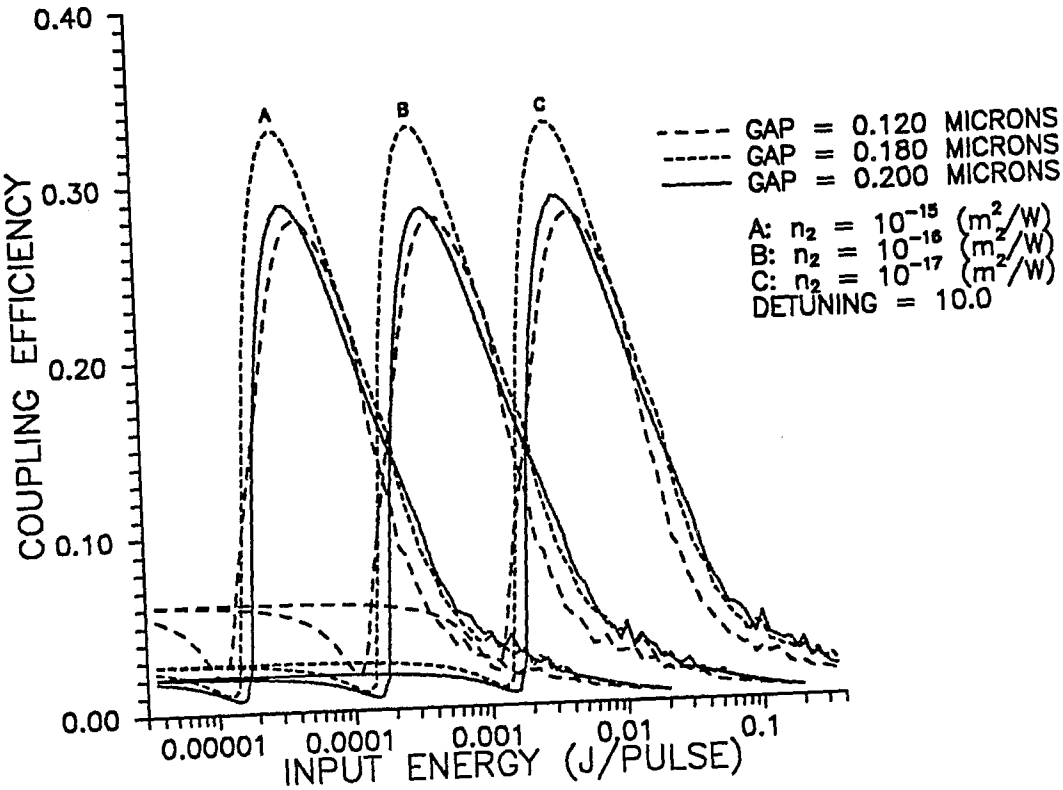

Figure 3.6. Coupling efficiency versus input energy for detuning of 10.0 and gap spacings of 0.12 μm, 0.18 μm, and 0.20 μm with Kerr law nonlinearities varying over 3 orders of magnitude.

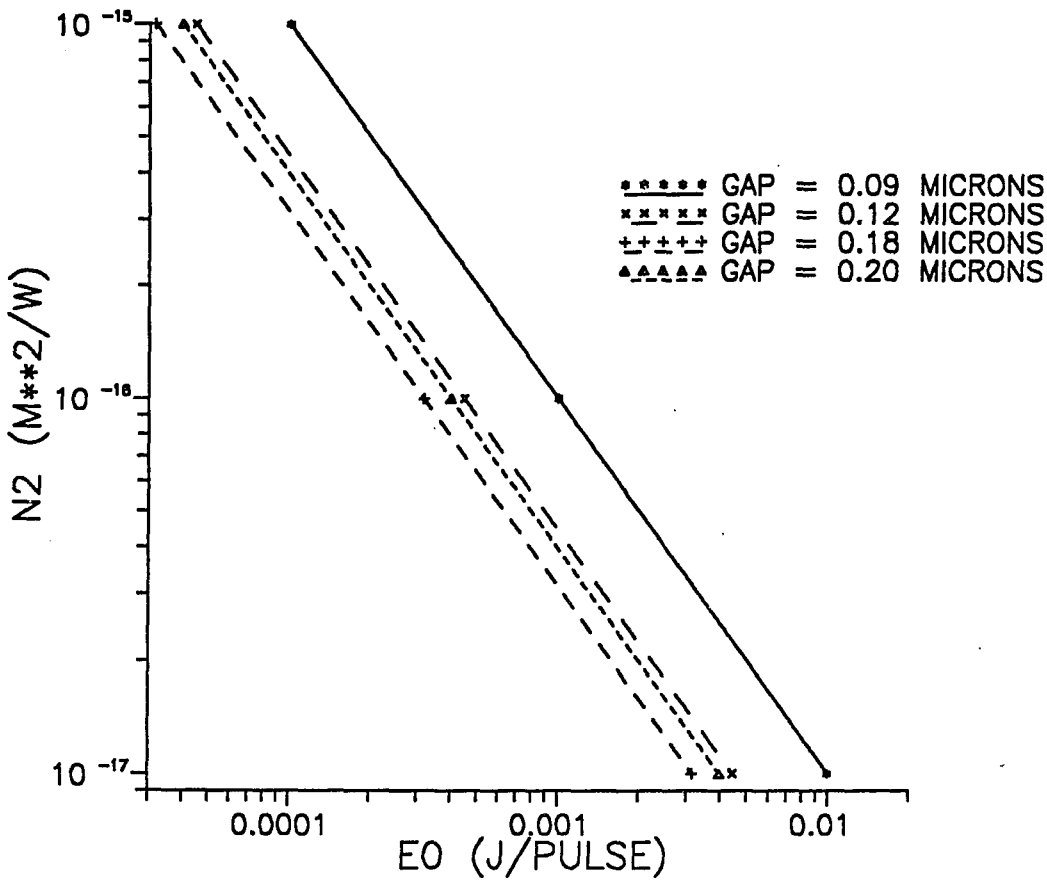

Figure 3.7. Kerr law nonlinear index, n_2 [units of m^2/w], versus input energy at peak efficiency, E_0, for detuning of 10.0 and gap spacings of 0.09 μm, 0.12 μm, 0.18 μm, and 0.20 μm.

CHAPTER FOUR

EXPERIMENTAL SETUP

The apparatus outlined in the schematic of figure 4.1 was constructed and test experiments carried out. A Quantel Corporation model 481 Nd:YAG laser, passively Q-switched with a saturable absorber dye (BDN - Exciton Chemical Company), produced 25 ns (FWHM) pulses of approximately Gaussian temporal profile. Radiation of wavelength λ = 1.064 μm at a repetition rate of 10 Hz was used to irradiate the waveguide. Laser power at the prism coupler was adjusted with a variable attenuator consisting of a motorized rotation stage and a polarization beam splitter cube which was used to set the proper polarization incident onto the prism coupler apparatus. Rotating the waveplate provided continuously variable attenuation that was computer controlled. A 500 mm focal length lens focused the beam to a spot size of w_0 = 1.31 mm (as measured with a Fairchild linear CCD array) at the input to the prism coupler.

Reverse-biased fast silicon PIN photodiodes (EG&G, model FND 100) were used to characterize both the reference and signal 25 ns pulses. Light falling onto the detectors was further attenuated using neutral density filters (Schott Glass Company) calibrated for use at 1.064 μm. Each detector was baffled to reduce spurious signals due to background radiation. A third photodiode captured a reflection from the back face of the polarizer and provided a trigger signal for the detection electronics.

Two different experiments were conducted on the same waveguide in attempts to observe nonlinear effects. In the first experiment, outputs from each

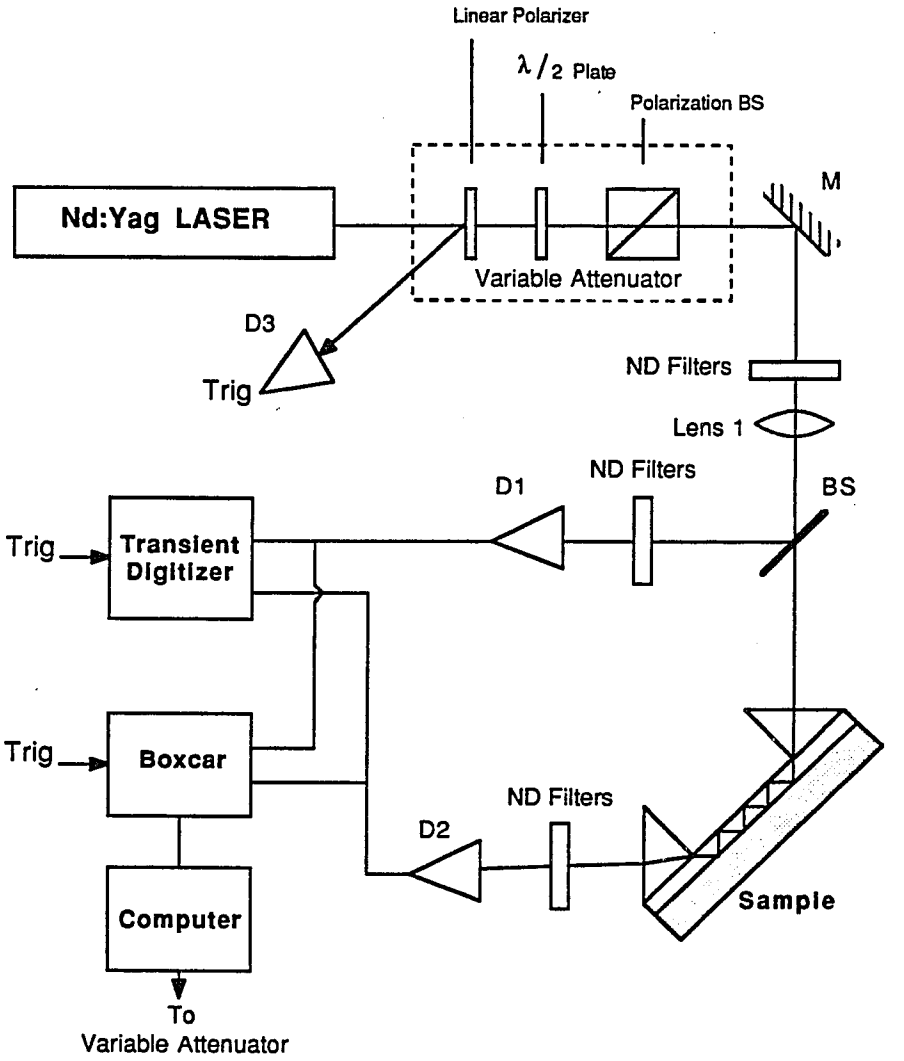

Figure 4.1. Schematic for nonlinear prism coupling apparatus. M = Mirror; BS = Beam Splitter; D1, D2, D3 are detectors; Trig = Trigger signal; ND Filters = Neutral Density Filters.

of the signal and reference detectors were fed into a boxcar integrator (Stanford Research Systems, model SR250) which integrated over the laser pulse. The reference detector was calibrated against a laser power meter (Scientech, model 365) and the signal detector was calibrated against the reference detector. A computer (IBM PC) was used to collect output voltage levels from the boxcar and to control laser beam attenuation through a stepper motor interface (Oriel, model 20010). At each power level the boxcar output was sampled over 50 pulses and an average voltage level assigned. All computer communication occurred via a standard RS-232 serial line. In the second experiment, signals from each detector were displayed on a transient digitizer with a 5 ns response time (Tektronix, model 7912AD). This allowed simultaneous display of individual pulses from both the waveguide input and output to facilitate the study of any pulse shape changes incurred in the waveguide. Digitized displays were photographed and peak voltages corresponding to peak powers were determined. Data are plotted as relative coupling efficiency versus input energy for both experiments.

The nonlinear waveguide was made by spin coating a polymer material onto a fused silica substrate. The polymer was obtained under a proprietary agreement with a commercial interest. Polymer powder was mixed 25% by weight in 1,2 dichloro-pentane and the resulting solution was filtered to remove particles larger than 0.2 μm. The solution was then spun onto a clean fused silica substrate (n_s = 1.450 at λ = 1.064 μm) at 1500 rpm and a uniform 1.6 μm thick film resulted. SF-6 glass prisms (n_p = 1.774) were carefully clamped to the top of the planar film. The film index was found by measuring the incoupling angles for the three guided modes seen with a cw helium neon laser at λ = 632.8 nm and then calculating the index from the theory of chapter 2. The film index was found to

be 1.619 ± 0.004. The waveguide was then characterized with the pulsed laser system.

CHAPTER FIVE

EXPERIMENTAL ANALYSIS AND DISCUSSION

The results of the coupling experiments are described in this chapter. After many attempts, a prism coupled waveguide that would couple and guide light at λ = 1.064 μm was finally made. Figure 5.1 shows data taken by averaging over the laser pulse with the boxcar averaging detection technique previously outlined. Each line and the corresponding points represent a separate data set taken one after the other while irradiating the same spot on the waveguide. The final energy for each successive run is slightly higher than the previous one. Energy is lost from reflection at each optical interface and by scattering and absorption within the waveguide. As a result, it is not possible with this technique to arrive at an absolute number for the guided-wave energy. Only relative changes in coupling efficiency are meaningful and the data are normalized to the largest value for output energy. The first data set appears to indicate a reduction of the coupling efficiency with increasing energy and hence a nonlinearity. This result, however, is not reproducible. With each return to low power the coupling efficiency drops and any curvature in the coupling efficiency curve is not reproducible. This shows that the waveguide has undergone a permanent change and some form of damage has occurred. The film probably heats up and melts, changing the index.

It is possible that reducing the number of laser pulses sent into the waveguide might alleviate this problem. With this experimental set-up, each data point is the average over 50 pulses. If each data run consists of approximately 25 data

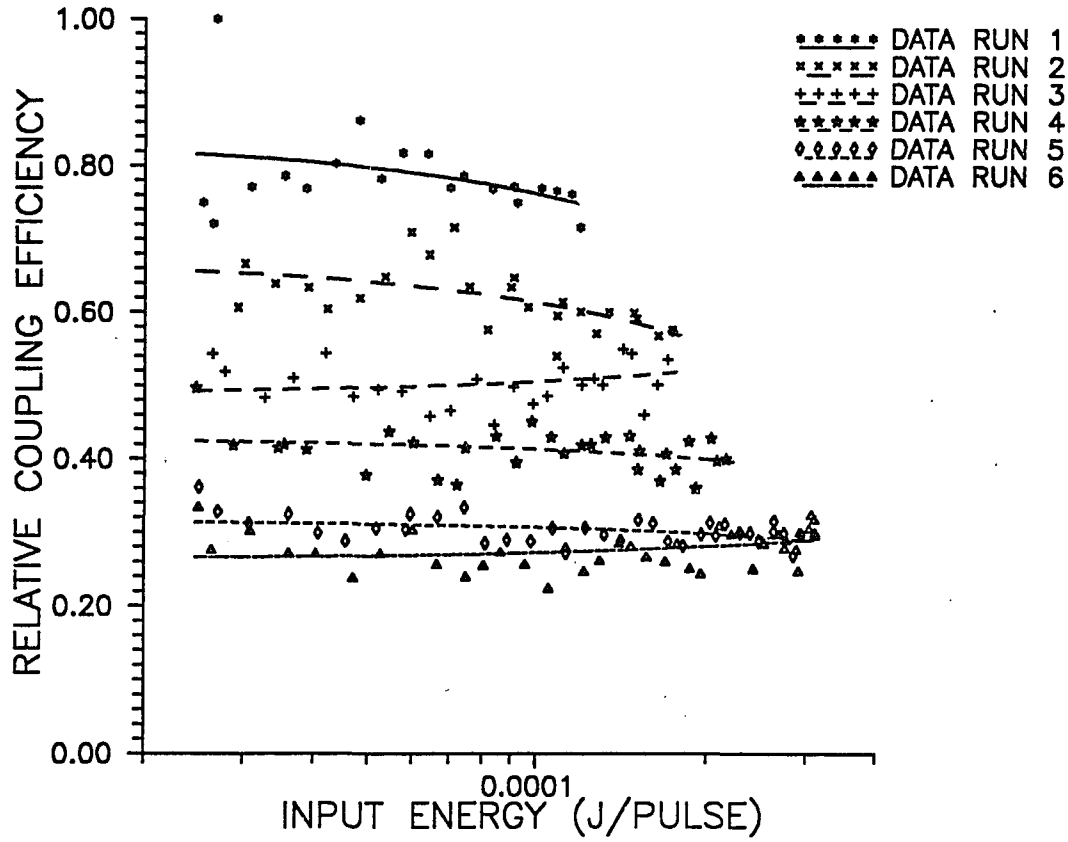

Figure 5.1. Relative coupling efficiency versus input energy for data taken using experimental technique 1.

points, allowing for time for the computer to increment the power, each data set allows the sample to be irradiated with upwards of 2000 pulses. This large quantity of energy absorbed must be dissipated by the film. Also, it was estimated that about one in ten pulses does not have a smooth pulse shape, but experiences what may be called "pulse break-up." A normal 25 ns wide Q-switch pulse at the input and output of a waveguide is shown in figure 5.2a. Figure 5.2b shows a pulse at the input and output that has "broken-up". Pulse break-up is caused by instabilities in the YAG laser that appear either through failure of the Q-switch dye to properly saturate or through thermally induced changes in the laser cavity dimensions. Figure 5.2b shows that pulse break-up produces one or more spikes at the input to the waveguide that have a large peak power and that do not appear at the output. This decreased coupling efficiency for these spikes indicates that damage to the waveguide may have occurred. Shuttering the beam to allow only those pulses with a clean profile through to the waveguide might reduce this problem.

A second set of experiments was performed in which both the number of pulses as well as the number of "bad" pulses was reduced. Starting at low power, pulses at the input and output to the waveguide were photographed simultaneously. Data were taken alternating between low and progressively higher energies to confirm the reproducibility of the peak heights. The beam was blocked between photos to reduce the number of pulses incident on the waveguide. Figure 5.3 shows the relative coupling efficiency versus input power found from the voltage peak heights in each of the photos. Although the data are noisy, no nonlinearity is seen right up to the damage point. Figure 5.3 also illustrates an alignment problem found with this set-up. During the course of the experiment

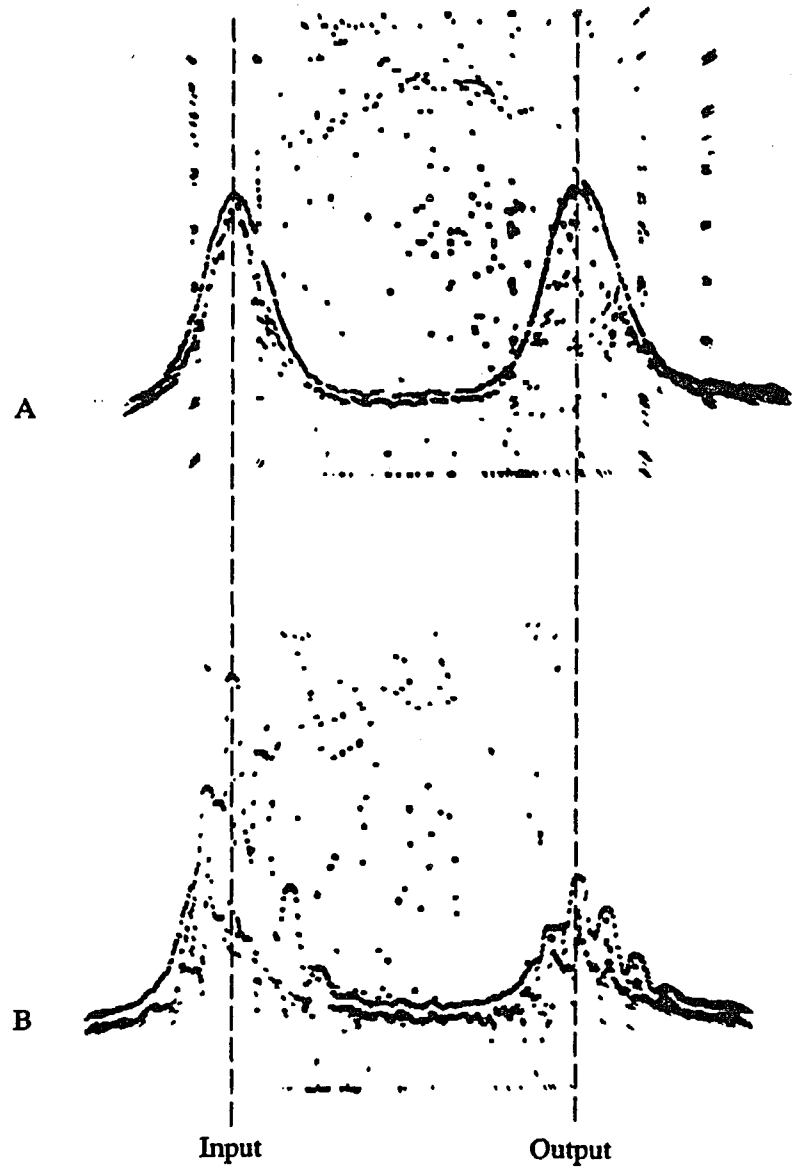

Figure 5.2. Laser pulse at the input and output of the prism coupled waveguide. a) Normal pulse shape. b) Pulse that has "broken-up." Horizontal scale is 20 ns per division for each.

the neutral density filter used to attenuate the beam at the waveguide input was removed. This shifted the beam enough to degrade the coupling efficiency. The waveguide position was readjusted and a large jump in the efficiency was seen. This shows that even small changes in the beam position, perhaps caused by thermal effects in the laser cavity, can degrade the coupling efficiency. Continous readjustment and optimization of the coupling appears to be necessary. Figure 5.4 illustrates evolution of the output pulse as the waveguide is damaged. At high powers, just before damage threshold, no reduction of coupling efficiency or changes in pulse shape that would indicate nonlinear phase changes in the waveguide are observed. Only after the damage threshold is reached does the output energy and hence the efficiency decrease.

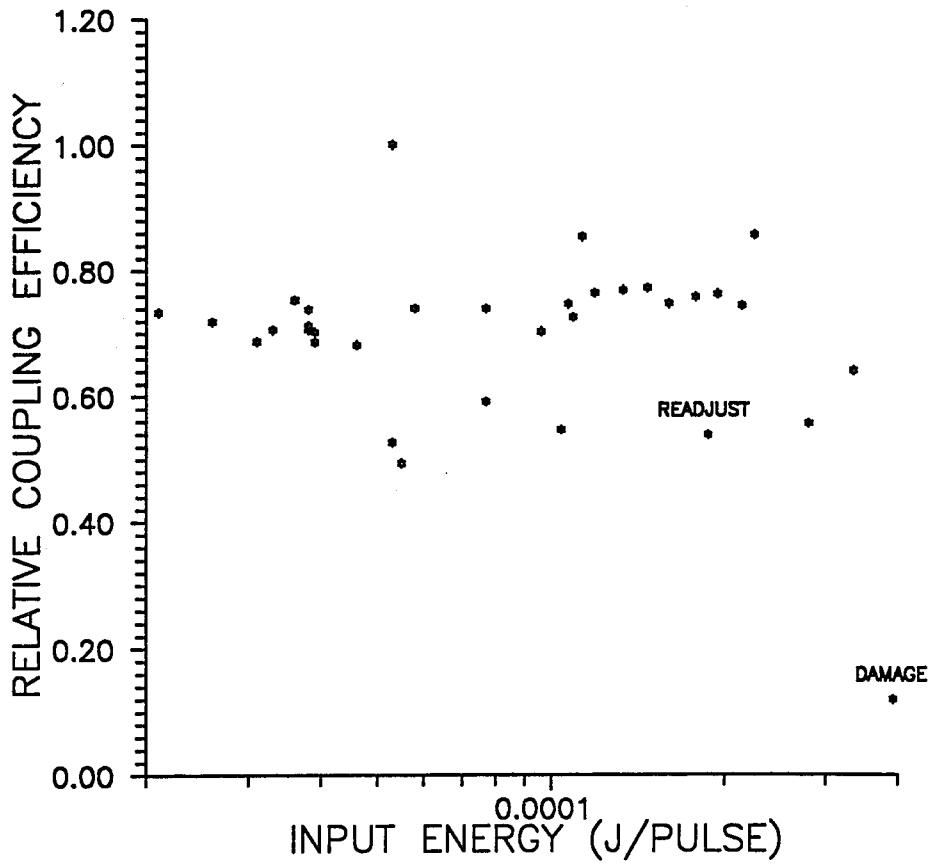

Figure 5.3. Relative coupling efficiency versus input energy for data taken for individual pulses with method 2.

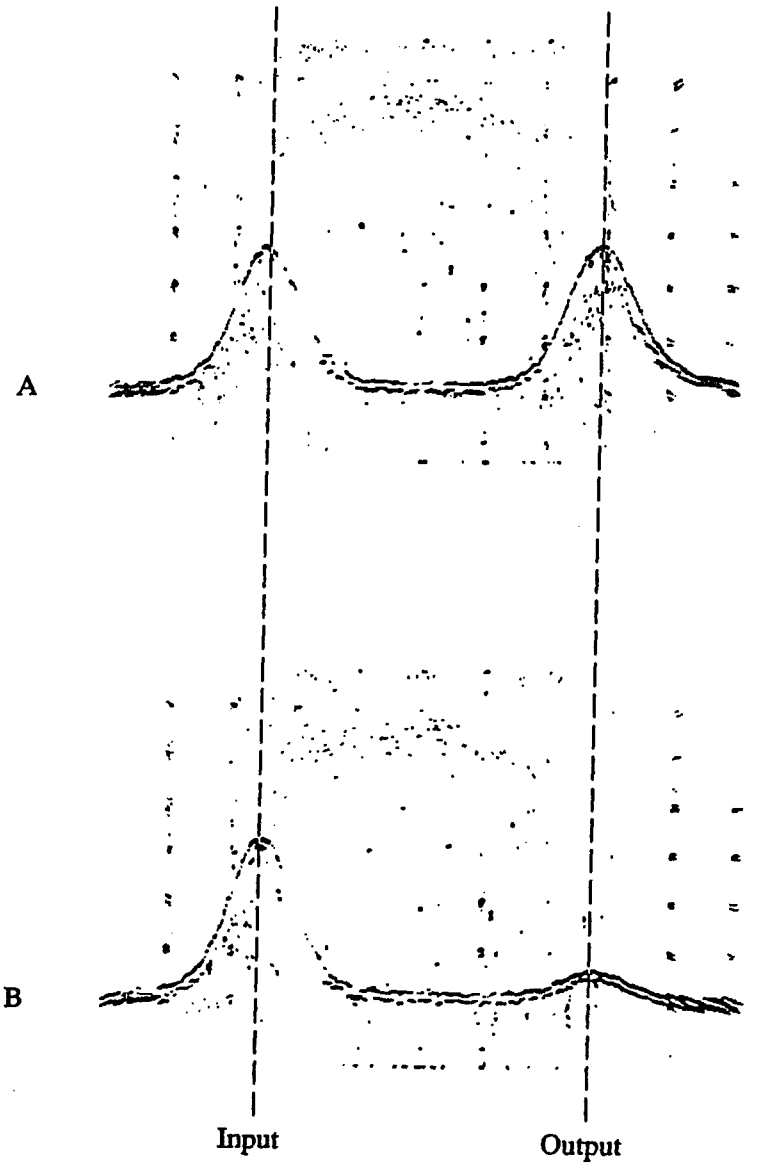

Figure 5.4. Pulse at input and output of waveguide for: A) energy just below the damage threshold; B) energy at damage threshold - damage has occurred; (continued on next page).

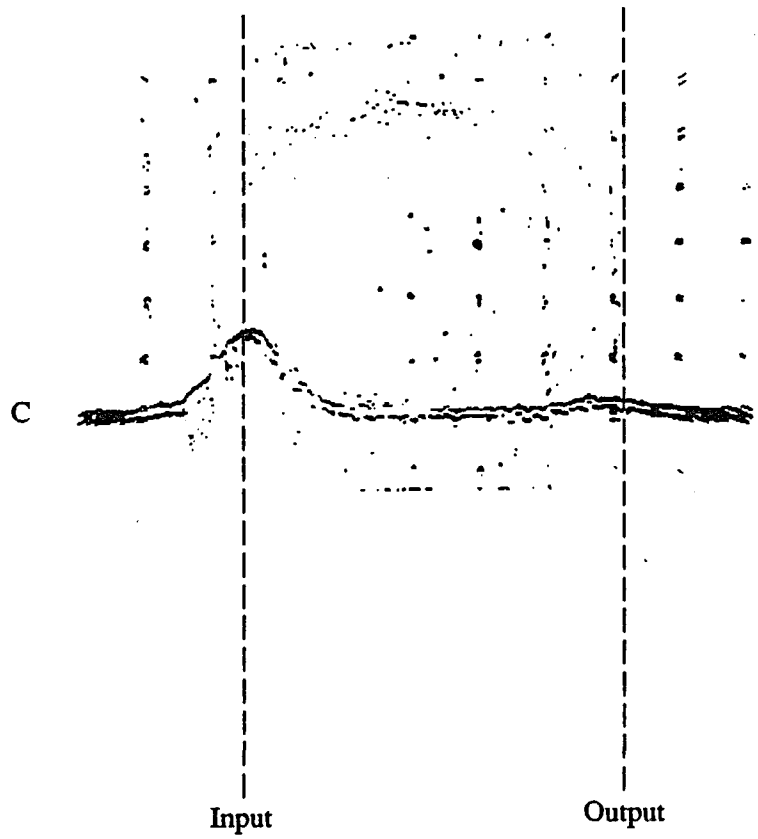

Figure 5.4. (continued), C) Pulse at input and output of waveguide for low incident energy - impossible to return to maximum coupling efficiency.

CHAPTER SIX

CONCLUSION

These numerical and experimental results indicate that finding an accurate value for n_2 using the prism coupling technique is a difficult problem. Several variables, some of which are difficult to measure, must be known before n_2 can be found. Provided that all of the other coupling parameters such as beam waist, beam position with respect to the prism edge, and detuning from optimum low power coupling angle can be carefully controlled, uncertainties in the gap dimension and its uniformity leads to uncertainties in the measurement of n_2. If an optimum gap is assumed then the actual n_2 value will be greater than or equal to the "measured" n_2 and the error in this estimate will be proportional to the uncertainty in the gap parameters. Other practical experimental problems such as laser alignment and detector alignment along with laser pulse instabilities contribute to the error in any measured value of n_2.

Despite these problems it is possible to evaluate n_2 experimentally. The inability to detect any nonlinear effects here indicates either that this polymer has an n_2 which is too small to detect, or that the experimental techniques must be improved. This technique has been used to observe thermal switching in polystyrene using microsecond pulses from a Nd:YAG laser (Assanto et al., 1988). However, no thermal switching was observed here using nanosecond pulses. A more carefully controlled experiment that allows observation of nonlinearities before the waveguide is damaged needs to be designed.

Appropriate changes in the design of the experiment should improve the results. Elimination of the prisms in favor of gratings as a means of distributive coupling into thin film waveguides would remove most of the uncertainties in the geometrical parameters of the guide. Gratings can be tailored to a specific application and the technology for making well-characterized gratings on glass substrates is developing fast. A stable and reliable YAG laser with a clean Gaussian spatial and smooth Gaussian temporal profile of less than 10 ns in width and adequate peak power is necessary to get reproducible results. In addition, an alignment helium neon laser (λ = 0.6328 μm) that is collinear with the YAG beam should be used to facilitate optimization of waveguide alignment and coupling efficiency at a visible wavelength. If prisms must be used, it may be possible to adjust the input prism clamping pressure to change the gap spacing. When the intensity of the specular reflection from the input prism decreases the light coupled into the prism increases and the gap will be close to optimum. With these changes the technique for relating coupling efficiency to input energy may yield useful numbers with an acceptable error in n_2. Clearly more work needs to be done before nonlinear prism coupling or nonlinear grating coupling can be used as an analytical tool to measure n_2.

REFERENCES

Assanto, G., Fortenberry, R.M., Seaton, C.T., Stegeman, G.I., "Theory of pulsed excitation of nonlinear distributed prism couplers," J. Opt. Soc. Am. B 5, 432 (1988).

Burzynski, R., Singh, B.P., Prasad, P.N., Zanoni, R., Stegeman, G.I.,"Nonlinear optical processes in a polymer waveguide: Grating coupler measurements of electronic and thermal nonlinearities," Appl. Phys. Lett., 53(21), 2011 (1988).

Carter, G., in *Nonlinear Optical Properties of Organic Molecules and Crystals*, Chemla, D., Zyss, J. eds., (Academic Press, New York, 1987).

Fortenberry, R.M., Assanto, G., Moshrefzadeh, R., Seaton, C.T., Stegeman, G.I., "Pulsed excitation of nonlinear distributed coupling into zinc oxide optical guides," J.Opt. Soc. Am. B 5, 425 (1988).

Hopf, F.A., Stegeman, G.I., *Applied Classical Electrodynamics Volume 1: Linear Optics*, (John Wiley & Sons, New York, 1985).

Kogelnik, H., in *Integrated Optics*, T. Tamir ed., (Springer-Verlag, New York, 1975).

Liao, C., Stegeman, G.I., Seaton, C.T., Shoemaker, R.L., Valera, J.D., Winful, H.G., "Nonlinear distributed waveguide couplers," J. Opt. Soc. Am. A 2, 590 (1985).

Munn, R.W., "Theory of molecular opto-electronics: from the molecule to the crystal," J. Molecular Electronics 4, 31 (1988).

Potember, R.S., Hoffman, R.C., Kim, S.H., Speck, S.R., Stetyick, K.A., "Molecular optical devices," J. Molecular Electronics 4, 5 (1988).

Shen, Y.R., *The Principles of Nonlinear Optics*, (John Wiley & Sons, New York, 1984).

Smith, P.W., "On the physical limits of digital optical switching and logic elements," Bell Sys. Tech. J. 61, 1975 (1982).

Stegeman, G.I., Seaton, C.T., Zanoni, R., "Organic films in nonlinear integrated optics structures," Thin Solid Films 152, 231 (1987).

Stegeman, G.I., Zanoni, R., Rochford, K., Seaton, C.T., "Third-order nonlinear guided-wave devices," Proc. of NATO Workshop on Nonlinear Optics in Polymers, Nice, 1988, in press.

Stegeman, G.I., Zanoni, R., Seaton, C.T., "Nonlinear organic materials in integrated optics structures," Mat. Res. Soc. Symp. **109**, 53 (1988).

Stegeman, G.I., Zanoni, R., Wright, E.M., Finlayson, N., Rochford, K., Ehrlich, J., Seaton, C.T., "Review of nonlinear integrated optics devices," Proceedings of Conference on Organic Materials for Nonlinear Optics, Oxford, 1988, in press.

Ulrich, R., "Theory of the prism-film coupler by plane-wave analysis," J. Opt. Soc. Am. **60**, 1337 (1970).